The Astrophysical Journal, 669:202–217, 2007 November 1

ON THE ORBIT STRUCTURE OF THE LOGARITHMIC POTENTIAL

C. Belmonte
Physics Department, University of Rome La Sapienza, Piazzale Aldo Moro 2, I00185 Rome, Italy; belmonte@roma1.infn.it
D. Boccaletti
Mathematics Department, University of Rome La Sapienza, Piazzale Aldo Moro 2, I00185 Rome, Italy; boccaletti@uniroma1.it
and
G. Pucacco[1]
Physics Department, University of Rome Tor Vergata, Via della Ricerca Scientifica 1, I00133 Rome, Italy; pucacco@roma2.infn.it
Received 2007 May 7; accepted 2007 July 4

ABSTRACT

We investigate the dynamics in the logarithmic galactic potential with an analytical approach. The phase-space structure of the real system is approximated with resonant detuned normal forms constructed with the method based on the Lie transform. Attention is focused on the properties of the axial periodic orbits and of low-order "boxlets" that play an important role in galactic models. Using energy and ellipticity as parameters, we find analytical expressions of several useful indicators, such as stability-instability thresholds, bifurcations, and phase-space fractions of some orbit families, and compare them with numerical results available in the literature.

Subject headings: galaxies: kinematics and dynamics — methods: analytical

1. INTRODUCTION

To determine salient features of the orbital structure of nonintegrable potentials is a fundamental topic in galactic dynamics. Knowledge of the existence and stability of periodic orbits of low commensurability is, for example, very important for clarifying the issue of triaxiality in elliptical galaxies, and a general understanding of the phase-space structure is very useful in applications of self-consistent models. The numerical approach is usually preferred due to the availability of reliable algorithms and powerful machines (Schwarzschild 1979; Merritt & Valluri 1996; Papaphilippou & Laskar 1996, 1998). However, in several circumstances it is useful to have some simple analytic clues concerning the relation between the form of the gravitational potential and the main families of orbits supported, as, for example, in the studies by Zhao et al. (1999).

Although generically nonintegrable, realistic galactic potentials show several properties of a regular behavior over wide energy ranges, with invariant surfaces ("tori") surrounding periodic orbits. Among these features, information about the stability properties of the main periodic orbits is of paramount importance, since the bulk of density distribution is shaped by the stars in regular phase-space domains around stable periodic orbits (Binney & Tremaine 1987). In particular, for triaxial ellipsoids, periodic orbits along symmetry axes play a special role. An enormous effort has therefore been devoted to investigate families and bifurcations of periodic orbits, starting with the study of models based on perturbed oscillators (Contopoulos 1970) and gradually exploring more realistic galactic potentials with numerical (Miralda-Escudé & Schwarzschild 1989; Fridman & Merritt 1997) and semianalytical (de Zeeuw & Merritt 1983; Scuflaire 1995) approaches. A related important problem is that of torus construction in the regular domains (Binney & Spergel 1982; Gerhard & Saha 1991; Kaasalainen & Binney 1994a, 1994b).

Techniques based on the various versions of perturbation theory have been applied to several examples and with different degrees of approximation (for a review, see, e.g., Contopoulos 2002). One of the most powerful analytic tools is the normal form approximation of a nonintegrable system. Although the normal form approach is quite widespread in galactic dynamics, its use in studying the stability of periodic orbits has not been as systematic as the theory could allow (Sanders & Verhulst 1985). The aim of the present paper is to apply the Lie transform normalization method (Hori 1966; Deprit 1969; Dragt & Finn 1976; Finn 1986; Koseleff 1994) to approximate the dynamics of the Binney logarithmic potential (Binney 1981). We compare the findings with that of Miralda-Escudé & Schwarzschild (1989), who employ purely numerical techniques to implement the Floquet method, and with that of Scuflaire (1995), who studies the stability of axial orbits by solving the Hill-like perturbation equation with the Lindstedt-Poincaré approach. Another example that is briefly mentioned is provided by the galactic Schwarzschild (1979) potential with a comparison to the results of de Zeeuw & Merritt (1983). These authors based their approach on the averaging procedure of normalization; it is therefore interesting to make a comparison with that method as well.

To study the structure of phase space with a truncated normal form, one may proceed in essentially two ways; the most general and exhaustive is that of determining the explicit form of periodic orbits and invariant tori that give the "skeleton" of the phase space of the system. A less general but easier approach in systems with 2 degrees of freedom (dof) is that of determining fixed points and invariant curves on a surface of section. This is constructed with the aid of the approximate integral of motion provided by the normalization. Even in the case of linear orbital stability of the main periodic orbits, the first method is in general quite cumbersome and can be applied when the procedure of reduction to a 1 dof Hamiltonian system and the use of action-angle variables lead to a reasonably simple system of equations. This reduction is always possible with 2 dof, both in the resonant and nonresonant cases (Gustavson 1966), whereas it is in general not possible in resonant systems with 3 dof. The second method is clearly less general but relies on straightforward geometric arguments related to the Hessian of a polynomial in its critical points and is, at

[1] Also at: INFN, Sezione di Roma Tor Vergata.

least in principle, quite easy to implement. In this work we apply both methods to perform the comparison mentioned in the paragraph above. There is another motivation to linger on both visions of the approximate dynamics: the normal form Hamiltonian is, in many respects, the "simplest" integrable relative of the nonintegrable original one. However, this simplicity is attained at the price of a set of coordinate transformations that deform the phase-space variables; if one is interested in specific local properties or wants to make comparison with numerical simulations, the inversion to the original variables becomes mandatory. Therefore, we want to deepen the relation between the "clean" but deformed dynamics provided by the normalizing variables and the dynamics in the physical variables "dirtied" by the inverse transformation.

Even in realistic potentials, the periodic orbits along the axes of symmetry (axial orbits) are easily identified both as normal modes of the reduced system and as "central" fixed points on the surfaces of section. Therefore, we limit the detailed evaluation of the stability characteristics in the parameter space to these axial orbits. However, both procedures we have followed are quite general and can be directly applied to all periodic orbits of sufficiently low commensurability. From the results obtained, we can state that the predictive power of the normal form ranges well outside the neighborhood in which the expansion of the original Hamiltonian is performed. It is rather related to the extent of the asymptotic convergence radius of the approximate integrals of motion, namely, the extent to which the remainder of the series truncated at a given order is minimal (see, e.g., Efthymiopoulos et al. 2004). The results suggest that there is still room for improvement up to a certain *optimal* order of truncation. Therefore, at least in the cases we have examined, the regular dynamics of a nonintegrable system can be reproduced with very high accuracy. However, in concrete applications the validity of the prediction has to be corroborated with an independent evaluation of the best-suited resonant normal form for the problem at hand, always bearing in mind that, after the onset of chaos, these methods become ineffective.

The plan of the paper is as follows. In § 2 we recall the procedure of normalization as applied to reflection symmetry potentials and state a criterion for the choice of the best-suited resonant normal form. In §§ 3 and 4 we study the 1:1 and 1:2 resonances, respectively. In § 5 we compare our analytical results with those available in the literature. In § 6 we sketch the conclusions.

2. ANALYTICAL SETUP

The normal form approach to investigate Hamiltonian systems has a wide range of applications in the astrophysical context. However, the method based on Lie transforms, which has several computational virtues with respect to the original methods (Gustavson 1966; Contopoulos 2002), has seldom been employed in galactic dynamics. Notable exceptions are the papers by Gerhard & Saha (1991) and Yanguas (2001) concerning perturbed isochrone models.

In this section we recall the most relevant mathematical tools, with the aim of laying down the notations and the main formulae. For a detailed account of the method, we refer to textbooks (Sanders & Verhulst 1985; Meyer & Hall 1992; Boccaletti & Pucacco 1999).

2.1. *General*

Suppose the system under investigation is given by a Hamiltonian

$$H(\boldsymbol{p},\boldsymbol{q}) = \frac{1}{2}\left(p_x^2 + p_y^2\right) + V\left(x^2, y^2\right), \tag{1}$$

where V is a smooth potential with an absolute minimum in the origin and reflection symmetry with respect to both axes. We expand the potential in the form

$$V(x,y;\varepsilon) = \sum_{k=0}^{\infty} \varepsilon^k V_k(x,y) \tag{2}$$

and look for a new Hamiltonian given by

$$K(\boldsymbol{P},\boldsymbol{Q};\varepsilon) = \sum_{n=0}^{\infty} \varepsilon^n K_n(\boldsymbol{P},\boldsymbol{Q}) = M_g^{-1} H(\boldsymbol{p},\boldsymbol{q};\varepsilon), \tag{3}$$

where $\boldsymbol{P}$ and $\boldsymbol{Q}$ result from the canonical transformation

$$(\boldsymbol{P},\boldsymbol{Q}) = M_g(\boldsymbol{p},\boldsymbol{q}). \tag{4}$$

In these and subsequent formulae we adopt the convention of labeling the first term in the expansion with the index zero; in general, the "zeroth-order" terms are quadratic homogeneous polynomials, and terms of order n are polynomials of degree $n+2$. The linear differential operator M_g is defined by

$$M_g \equiv e^{-\varepsilon L_{g_1}} e^{-\varepsilon^2 L_{g_2}} \ldots e^{-\varepsilon^n L_{g_n}} \ldots = \sum_{n=0}^{\infty} \varepsilon^n M_n. \tag{5}$$

The functions g_n are the coefficients in the expansion of the generating function of the canonical transformation, and the linear differential operator L_g is defined through the Poisson bracket

$$L_g f \equiv \{g,f\} \equiv \frac{\partial g}{\partial x}\frac{\partial f}{\partial p_x} + \frac{\partial g}{\partial y}\frac{\partial f}{\partial p_y} - \frac{\partial g}{\partial p_x}\frac{\partial f}{\partial x} - \frac{\partial g}{\partial p_y}\frac{\partial f}{\partial y}. \tag{6}$$

The exponentials in the definition of M_g are intended as the *formal* sum of a power series so that it gives rise to a near-identity coordinate transformation known as a *Lie series*. Therefore, in practice, in the algorithm implemented to compute the K_n appearing in equation (3), what are really used are the differential operators

$$M_n = \sum_{m_1+2m_2+\ldots nm_n=n} \frac{L_{g_1}^{m_1} L_{g_2}^{m_2} \ldots L_{g_n}^{m_n}}{m_1! m_2! \ldots m_n!}. \tag{7}$$

By expanding also the right-hand side of equation (3) in power series of ε and equating the coefficients of the same order, one has the recursive set of linear partial differential equations

$$\begin{aligned} K_0 &= H_0 = \frac{1}{2}\left(p_x^2 + p_y^2\right) + V_0, \\ K_1 &= V_1 + M_1 H_0, \\ &\vdots \\ K_n &= V_n + M_n H_0 + \sum_{m=1}^{n-1} M_{n-m} V_m, \\ &\vdots \end{aligned} \tag{8}$$

It can be seen that each equation in the chain from equation (8) depends only on quantities found in the previous line. "Solving"

the equation at the nth step consists of a twofold task: finding K_n *and* g_n. The unperturbed part of the Hamiltonian, H_0, determines the specific form of the transformation. In fact, the new Hamiltonian K is said to be *in normal form* if

$$\{H_0, K\} = 0. \tag{9}$$

This condition is used at each step of the procedure to determine the functions g_n in order to eliminate as many terms as possible in the new Hamiltonian. The only terms of which K is made of are those staying in the kernel of the operator L_{H_0} associated with H_0 through the definition from equation (6). The procedure is stopped at some "optimal" order N, and therefore, in all ensuing discussion we refer to a "truncated" normal form. H_0 must be considered as a function of the new coordinates at each step in the process: according to equation (9), it is therefore an integral of the motion for the new Hamiltonian K. The function

$$\mathcal{I} = K - H_0 \tag{10}$$

can be therefore used as a second integral of motion conveying approximate information on the dynamics of the original system.

The normalizing transformation from equation (4) leads to new coordinates which are continuous differentiable *deformations* of the original ones. For practical applications (for example, to compare results with numerical computations), it is useful to express approximating functions in the original physical coordinates. Inverting the coordinate transformation, the new integral of motion can be expressed in terms of the original variables. Denoting it as the power series

$$I = \sum_{n=0}^{\infty} \varepsilon^n I_n, \tag{11}$$

its terms can be recovered by means of

$$I_n = V_n - K_n + \sum_{m=1}^{n-1} M_{n-m}(V_m - I_m), \quad n \geq 1, \tag{12}$$

which is obtained from equation (10) by exploiting the nice properties of the Lie transform with respect to inversions (Boccaletti & Pucacco 1999).

It is important to remember in which respect the normal form K and the integral I provide approximations to the dynamics of the original system. The normal form is truncated at step N: this means that in the new Hamiltonian a "remainder" of order $O(\varepsilon^{N+1})$ is neglected and the two functions K and $\mathcal{I}$ provide an (exactly) integrable system whose dynamics, in the new coordinates, is within $O(\varepsilon^N)$ of the original system. On the other hand, inverting the canonical normalizing transformation, the power series from equation (11) is an approximate integral of motion of the original system (in the original coordinates), since

$$\{I, H\} = O\left(\varepsilon^{N+1}\right). \tag{13}$$

That is, I fails to commute with the original Hamiltonian for terms of higher order. We see that in both cases the error made with the perturbative method is of the same amount, since terms of the same order are neglected. However, it is not clear if, in the case of high orders and when a direct comparison is possible, both approaches lead exactly to the same predictions. Since in various applications one or the other approaches have pros and cons, one of the aims of the present work is just to examine and reconcile possible discrepancies.

We remark that in all subsequent applications involving series expansions, the role of the perturbation parameter can also be played by the size of the neighborhood of the origin where the Hamiltonian is considered. Therefore, the powers of the parameter ε are left in all expansion formulae just to indicate their order and are treated as unity in the computations.

2.2. *Expanding "Cored" Galactic Potentials*

The model potential we consider is the Binney logarithmic potential (Binney & Tremaine 1987). The logarithmic potential has played a fundamental role in the description of galactic models displaying, with a very simple analytical expression, many realistic features of elliptical galaxies, in particular employing its singular scale-free form (Miralda-Escudé & Schwarzschild 1989)

$$V = (1/2)\log\left(x^2 + y^2/q^2\right). \tag{14}$$

We cannot apply the standard normalization procedure as it is to a singular potential. In this way we are still not able to explore the phase-space structure of cuspy models that nowadays seem to be required by the observed properties of real galaxies (Merritt 1999). However, selected classes of power-law or other singular potentials can be put in a form suitable to the normalization algorithm by a proper coordinate transformation (Sridhar & Touma 1997). Moreover, it is important to remark that the class of "weak" cusps (Dehnen 1993) displays many features of cored potentials, as can be seen in the numerical exploration performed by Fridman & Merritt (1997). Therefore, the analysis presented here, even if restricted to potentials that can be Taylor expanded around a homogeneous density core, is a useful starting point. Enforcing the reflection symmetries of galactic potentials, we assume that each term in the expansion from equation (2) can be written as a homogeneous polynomial of degree $2(k+1)$ of the form

$$V_{2k}(x,y) = \frac{1}{2(k+1)} \sum_{j=0}^{k+1} a_{2(j,k-j+1)} x^{2j} y^{2(k-j+1)}, \quad k = 0, 1, 2, \ldots. \tag{15}$$

A Taylor expansion has a convergence radius that can be finite and small if compared with the region of interesting dynamics. One could conservatively deduce that the normal form is a good approximation of the dynamics only *within* the convergence radius of the potential. However, things are not so simple, because what really matters is the convergence of the normal form itself. In fact, it may happen that a potential with infinite convergence radius, for example, a perturbed oscillator without escape, has a normal form with a finite convergence radius; usually, this is related to the breakup of regular dynamics and the transition to stochasticity. Clearly, in this case there is no hope to get reliable information on the dynamics beyond the stochasticity threshold from the normal form. On the opposite side, there is the possibility that the system, even if nonintegrable, displays regular dynamics almost everywhere, and in this case, the normal form can be used even *outside* the convergence radius of the original potential. The logarithmic potential offers the opportunity to explore all these issues (Kaasalainen & Binney 1994b).

The cored logarithmic potential can be written as

$$V = (1/2)\log\left(1 + x^2 + y^2/q^2\right). \tag{16}$$

The form written here is simplified by the choice of fixing the length scale (the "core radius" R_c) equal to one, but this is not a limitation due to the invariance in both the length scale and the

energy scale. With these units, the energy E may take any nonnegative value,

$$0 \leq E < \infty. \tag{17}$$

The parameter giving the "ellipticity" of the figure ranges in the interval

$$0.6 \leq q \leq 1. \tag{18}$$

Lower values of q can in principle be considered, but correspond to a nonphysical density distribution. Values greater than unity are included in the treatment by reversing the role of the coordinate axes, effectively extending the range to the upper limit $1/0.6 = 5/3$. The series expansion of the logarithmic potential is

$$V = \frac{1}{2}\sum_{k=0}^{\infty}\frac{(-1)^k}{k+1}\left(x^2+\frac{y^2}{q^2}\right)^{k+1}, \tag{19}$$

so that the coefficients appearing in equation (15) are

$$a_{2(j,k-j+1)} = \binom{k+1}{j}\frac{(-1)^k}{q^{2(k-j+1)}}. \tag{20}$$

Those of lowest order are

$$a_{(2,0)} = \omega_1^2 = 1, \quad a_{(0,2)} = \omega_2^2 = 1/q^2, \tag{21}$$

$$a_{(4,0)} = -1, \quad a_{(2,2)} = -2/q^2, \quad a_{(0,4)} = -1/q^4, \tag{22}$$

$$a_{(6,0)} = 1, \quad a_{(4,2)} = 3/q^2, \quad a_{(2,4)} = 3/q^4, \quad a_{(0,6)} = 1/q^6. \tag{23}$$

The natural setting in which one performs a low-order normalization according to the definition from equation (9) is therefore that of a perturbed quadratic Hamiltonian with a potential starting with the harmonic term and "frequencies" given by equation (21). For a generic value of q, the frequency ratio

$$\omega_1/\omega_2 \equiv q \tag{24}$$

is a real number; the frequencies are rationally independent, and the terms in the normal form, that is, those polynomials in the canonical variables commuting with

$$H_0 = (1/2)\left(p_x^2 + p_y^2 + \omega_1^2 x^2 + \omega_2^2 y^2\right), \tag{25}$$

consist only of functions of the partial energies in the harmonic potential. It is customary to refer to the normal form constructed in this case as a "Birkhoff" normal form (Birkhoff 1927). The presence of terms with small denominators in the expansion forbids in general its convergence. It is therefore more effective to work from the start with a *resonant normal form* (Sanders & Verhulst 1985), which is still nonconvergent, but has the advantage of avoiding the small divisors associated with a particular resonance. To catch the main features of the orbital structure, we therefore approximate the frequencies with a rational number plus a small "detuning" that we assume to be of $O(\varepsilon^2)$,

$$\omega_1/\omega_2 = q = (m/n) + \varepsilon^2\delta. \tag{26}$$

We speak of a *detuned* $(m:n)$ *resonance*, with $m+n$ the *order* of the resonance. The algorithm to perform a resonant normalization generalizes that of the Birkhoff normalization in its ability to identify additional terms to be included in the normal form, since they cannot be eliminated with the sequence of canonical transformations. To this end, the system must be in a form suitable to apply the resonant normalization procedure; we rescale variables according to

$$x \longrightarrow \sqrt{\omega_1}x, \quad y \longrightarrow \sqrt{\omega_2}y, \quad p_x \longrightarrow \frac{p_x}{\sqrt{\omega_1}}, \quad p_y \longrightarrow \frac{p_y}{\sqrt{\omega_2}}, \tag{27}$$

in order to put the Hamiltonian in the form

$$\mathcal{H} = \frac{1}{2}\left[\left(m+n\varepsilon^2\delta\right)\left(p_x^2+x^2\right)+n\left(p_y^2+y^2\right)\right] + \sum_{k=1}^{\infty}\frac{\varepsilon^{2k}}{2(k+1)}\sum_{j=0}^{k+1}b_{2(j,k-j+1)}x^{2j}y^{2(k-j+1)}, \tag{28}$$

where we have used the same notation for the rescaled variables and

$$b_{2(j,k-j+1)} = \frac{n a_{2(j,k-j+1)}}{\omega_1^j\omega_2^{k-j+2}}. \tag{29}$$

Frequencies have been approximated as in equation (26), and the Hamiltonian is redefined according to the rescaling

$$\mathcal{H} \equiv nH/\omega_2 = nqH. \tag{30}$$

As before, the new Hamiltonian K is said to be in normal form if

$$\{\mathcal{H}_0, K\} = 0, \tag{31}$$

where in agreement with equation (30), the unperturbed part of the Hamiltonian from equation (25) has been replaced by

$$\mathcal{H}_0 = \frac{1}{2}\left[m\left(p_x^2+x^2\right)+n\left(p_y^2+y^2\right)\right] \tag{32}$$

and the procedure is now that of an ordinary resonant "Birkhoff-Gustavson" normalization (Gustavson 1966; Moser 1968) with two variants: the coordinate transformations are performed through the Lie series and the detuning quadratic term is treated as a term of higher order and put in the perturbation.

2.3. *Choice of the Resonance*

The "skeleton" of the regular part of the phase space of a nonintegrable system is framed by periodic orbits and invariant tori. In particular, knowing the location and stability of periodic orbits allows one to gather a substantial piece of information concerning the whole dynamics. Moreover, determining the instability thresholds in terms of physical parameters (e.g., the energy) also provides clues on the extent to which stochasticity becomes important. The change in stability of a periodic orbit is connected to frequency ratios; commensurability of low orders between frequencies is the main trigger to stability-instability transition, and the interaction of resonances provides chaos. In harmonic oscillators, frequency ratios are fixed; if their ratio is nonrational, there is no resonance. For example, the quadratic part of the logarithmic potential is given by the coefficients from equation (21); with q in the range from

equation (18), there is no reason to assume it to be a rational number. However, coupling between the dof due to the perturbation causes the frequency ratios to change. The system *passes through* resonances of order given by the integer ratios closest to the ratio of the unperturbed frequencies. Crossing the resonance, a stability change may occur, and in general, a new sequence of periodic orbits bifurcates (Merritt 1999; Contopoulos 2002). Given an arbitrary pair of unperturbed frequencies, it could seem better to approximate their ratio as close as possible with integers. However, there is an argument on which a more effective choice can be based. A typical situation is that in which a family of periodic orbits becomes unstable when a low-order resonance occurs between its fundamental frequency and that of a normal perturbation; the simplest case is given by an axial orbit that, depending on the specific form of the potential, can be unstable through bifurcation of loop orbits (1:1 resonance), "banana" orbits (1:2 resonance), "fish" orbits (2:3 resonance), etc. Therefore, a detuned low-order resonant normal form can be quite accurate in describing the corresponding bifurcations. The strategy can be either a systematic exploration of the hierarchy of resonances or a specific choice guided by some independent argument (energy range, ellipticity range, etc.). Clearly, since the frequency ratio from equation (26) is given by the parameter q that determines the shapes of the isopotentials, fixing a specific value of q in the range from equation (18) also indicates which resonance is expected to be closer.

It must be emphasized that the structure of a resonant normal form is also affected by the symmetries of the original system. The normal form must preserve these symmetries, and this in general also leads to a criterion for truncation. In the present instance of a double reflection symmetry, given a resonance ratio m/n, the normal form must contain at least terms of degree $2(m+n)$ (see, e.g., Tuwankotta & Verhulst 2000). Therefore, the criterion we have adopted in this paper has been that of starting with the lowest order truncated normal form incorporating the symmetries of a typical galactic potential. A systematic investigation of the optimal order of truncation has recently been performed by Contopoulos et al. (2003) and Efthymiopoulos et al. (2004). Their results confirm the rapid decrease of the optimal order with the radius of the phase-space domain in which expansions are computed; we may conjecture that if we are interested in the global dynamics and accept a moderate level of accuracy, with this very conservative approach we can get reliable information up to the breakdown of the regular dynamics. Once particular orbits (or other interesting features) of the system are selected, more accurate details concerning the location, stability thresholds, and so forth can be derived with a higher order truncation.

3. 1:1 SYMMETRIC RESONANCE AND SECOND-ORDER NORMALIZATION

We proceed by exploiting the normal form of the system with the Hamiltonian from equation (28), the potential from equation (19), and the prescription from equation (29), starting with the simplest possibility: a Lie transform normalization truncated to the first nonnull term in the normal form. Recalling the symmetries of the potential represented by equation (21), the first nontrivial equation in the chain from equation (8) is

$$K_2 = V_2 + M_2\mathcal{H}_0, \tag{33}$$

so that we actually truncate at order 2. Applying standard methods (Meyer & Hall 1992; Boccaletti & Pucacco 1999) gives the following expression of the second-order normal form (Belmonte et al. 2006):

$$K_2^{(1:1)} = \frac{1}{2}\delta\left(P_X^2+X^2\right) - \frac{3}{32}\left[q\left(P_X^2+X^2\right)^2 + \frac{1}{q}\left(P_Y^2+Y^2\right)^2\right] - \frac{1}{16}\left[P_Y^2\left(3P_X^2+X^2\right) + Y^2\left(P_X^2+3X^2\right) + 4P_XP_YXY\right], \tag{34}$$

$$K_2^{(m:n)} = \frac{n}{2}\delta\left(P_X^2+X^2\right) + k_1\left[q\left(P_X^2+X^2\right)^2 + \frac{1}{q}\left(P_Y^2+Y^2\right)^2\right] + k_2\left(P_X^2+X^2\right)\left(P_Y^2+Y^2\right), \tag{35}$$

where the values of the coefficients in the expansion of the potential come from equations (21) and (22), and k_1 and k_2 are rational numbers dependent on m and n. Equation (26) has been used, and the canonical variables $\boldsymbol{P}$ and $\boldsymbol{Q}$ are as in equation (3). We see that this case behaves in the same way as in the first-order–averaging approach (de Zeeuw & Merritt 1983; Verhulst 1996): the 1:1 resonance *or all other resonances*. This remark is another clue to the strategy delineated in § 2.3, which is to limit the global analysis to a normal form truncated to the first term incorporating a meaningful resonance. Therefore, for a preliminary investigation of periodic orbits with the lowest commensurability, which in the present instance is

$$\omega_1/\omega_2 = 1 + \varepsilon^2\delta, \tag{36}$$

we can just exploit a 1:1 normal form truncated at $K_2^{(1:1)}$.

In the following subsections we work out in detail this analysis to take it also as a record for the cases with higher order resonances. In fact, in these cases the procedure goes along the same lines, but reporting computations in details is not so easy due to huge expressions. In § 5.1 we get more accurate numerical results going to sixth order. A detailed study of the orbits in the 1:1 resonance case (including periodic and nonperiodic orbits) has been provided by Contopoulos (1965).

3.1. *Orbit Structure of the 1:1 Resonance*

To investigate the phase-space structure of the system, it is convenient to write the normal form as

$$K^{(1:1)} = J_1 + J_2 + \varepsilon^2\left(\delta J_1 - \frac{3}{8}\left\{qJ_1^2 + \frac{1}{q}J_2^2 + \frac{2}{3}J_1J_2\left[2+\cos\left(2\theta_1-2\theta_2\right)\right]\right\}\right), \tag{37}$$

where the action-angle variables are introduced according to

$$X = \sqrt{2J_1}\cos\theta_1, \tag{38}$$

$$P_X = \sqrt{2J_1}\sin\theta_1, \tag{39}$$

$$Y = \sqrt{2J_2}\cos\theta_2, \tag{40}$$

$$P_Y = \sqrt{2J_2}\sin\theta_2. \tag{41}$$

The structure of equation (37) displays the effect of the symmetries on the resonant part: angles appear only through the combination $2\theta_1 - 2\theta_2$, and this shows why the symmetric 1:1 resonance can also be dubbed a "2:2" resonance. We now have an integrable system with dynamics generated by the Hamiltonian from equation (37) with a second independent integral of motion

$$\mathcal{H}_0 \equiv \mathcal{E} = J_1 + J_2. \tag{42}$$

This system is the simplest integrable approximation of the nonintegrable dynamics in the logarithmic potential dominated by the lowest order resonance. In the normal form of equation (37), the perturbation parameter appears as a reminder to denote terms of the same order and, according to the criterion stated above (see § 2.1), is set equal to unity in the computations. To get a quick overview of its structure, we can use equation (37) to identify the main periodic orbits. The procedure is the following (Sanders & Verhulst 1985, § 7.4): we perform the canonical transformation to "adapted resonance coordinates"

$$\psi = 2(\theta_1 - \theta_2), \tag{43}$$

$$\chi = 2(\theta_1 + \theta_2), \tag{44}$$

$$J_1 = (\mathcal{E} + \mathcal{R})/2, \tag{45}$$

$$J_2 = (\mathcal{E} - \mathcal{R})/2, \tag{46}$$

where $\mathcal{E}$ is defined in equation (42) and

$$\mathcal{R} = J_1 - J_2. \tag{47}$$

Since χ is cyclic and its conjugate action $\mathcal{E}$ is the additional integral of motion, we introduce the "effective" Hamiltonian

$$\tilde{K} = K^{(1:1)}(\mathcal{R}, \psi; \mathcal{E}, q), \tag{48}$$

namely,

$$\tilde{K} = \mathcal{E} + \frac{1}{2}(q-1)(\mathcal{E} + \mathcal{R}) + A\left(\mathcal{E}^2 + \mathcal{R}^2\right) + B\mathcal{E}\mathcal{R} + C\left(\mathcal{E}^2 - \mathcal{R}^2\right)(2 + \cos\psi), \tag{49}$$

with

$$A = -\frac{3(q^2+1)}{32q}, \tag{50}$$

$$B = -\frac{3(q^2-1)}{16q}, \tag{51}$$

$$C = -\frac{1}{16}. \tag{52}$$

Considering the dynamics at a fixed value of $\mathcal{E}$, we have that $\tilde{K}$ defines a 1 dof $(\psi, \mathcal{R})$ system with the equations of motion

$$\dot{\psi} = \tilde{K}_{\mathcal{R}} = \frac{1}{2}(q-1) + B\mathcal{E} + 2[A - C(2 + \cos\psi)]\mathcal{R}, \tag{53}$$

$$\dot{\mathcal{R}} = -\tilde{K}_{\psi} = C\left(\mathcal{E}^2 - \mathcal{R}^2\right)\sin\psi. \tag{54}$$

Let us determine the fixed points of this system; these in turn give the periodic orbits of the original system. The right-hand side of equation (54) vanishes in one of the following three cases:

1. $\mathcal{R} = \pm\mathcal{E}$,
2. $\psi = 0$,
3. $\psi = \pm\pi$.

In the first case, the right-hand side of equation (53) vanishes when

$$1 - q - 2\{B \pm 2[A - C(2 + \cos\psi)]\}\mathcal{E} = 0, \tag{55}$$

and the two periodic orbits

$$\mathcal{R} = \mathcal{E}, \quad J_2 = 0 \quad \text{(type Ia)}, \tag{56}$$

$$\mathcal{R} = -\mathcal{E}, \quad J_1 = 0 \quad \text{(type Ib)} \tag{57}$$

ensue. The orbit of type Ia is the periodic orbit along the x-axis (long axial orbit), whereas the orbit of type Ib is the periodic orbit along the y-axis (short axial orbit).

In the second case, the right-hand side of equation (53) vanishes when

$$\mathcal{R} = \frac{q - 1 + 2B\mathcal{E}}{4(3C - A)} = \frac{8q - 3(1+q)\mathcal{E}}{3(q-1)}, \quad \psi = 0, \tag{58}$$

where equations (50)–(52) have been used. This fixed point determines the "inclined" orbit

$$J_1 = \frac{4q - 3\mathcal{E}}{3(q-1)}, \quad J_2 = \frac{q(3\mathcal{E} - 4)}{3(q-1)} \quad \text{(type II)}. \tag{59}$$

Note that

$$0 \le J_1, J_2 \le \mathcal{E} \tag{60}$$

and this range determines the condition for existence of the orbit of type II.

In the third case, the right-hand side of equation (53) vanishes when

$$\mathcal{R} = \frac{q - 1 + 2B\mathcal{E}}{4(C - A)} = \frac{8q(q-1) + 3(1-q^2)\mathcal{E}}{3q^2 - 2q + 3}, \quad \psi = \pi. \tag{61}$$

The fixed point in equation (61) determines the elliptic ("loop") orbit

$$J_1 = \frac{(3-q)\mathcal{E} + 4q(q-1)}{3q^2 - 2q + 3},$$

$$J_2 = \frac{q(3q-1)\mathcal{E} - 4q(q-1)}{3q^2 - 2q + 3} \quad \text{(type III)}. \tag{62}$$

The range from equation (60) still determines the condition for existence of the orbit of type III.

3.2. *Stability Analysis of the 1:1 Resonance*

Let us now consider the question of the stability of the periodic orbits. As discussed in § 3.1, the 1 : 1 resonant normal form essentially captures those features of the system characterized by the lowest order of commensurability between frequencies. In particular, it is able to describe the cases in which the nominal frequency characterizing a periodic orbit happens to become equal to that of a normal perturbation. The characteristic curve representing this equivalence in some suitable parameter space provides the stability-instability transition looked for.

For orbits of types II and III, an ordinary investigation of the equations of variations of the system from equations (53) and (54) is enough to perform the linear stability analysis (Contopoulos 1978) in analogy with the Floquet method. However, in the case of axial orbits of type I, action-angle variables have singularities on them, and these also affect the adapted resonance coordinates. However, the remedy is quite straightforward: use a mixed combination of action-angle variables on the orbit itself and Cartesian variables for the other dof.

Let us start with the orbits of type II and III that, due to their nonsingularity, are usually referred to as *periodic orbits in general*

position. The system of differential equations for the perturbations $(\delta\psi, \delta\mathcal{R})$ is given by

$$\frac{d}{dt}\begin{pmatrix}\delta\psi\\ \delta\mathcal{R}\end{pmatrix}=\begin{pmatrix}\tilde{K}_{\mathcal{R}\psi} & \tilde{K}_{\mathcal{R}\mathcal{R}}\\ -\tilde{K}_{\psi\psi} & -\tilde{K}_{\mathcal{R}\psi}\end{pmatrix}\begin{pmatrix}\delta\psi\\ \delta\mathcal{R}\end{pmatrix}. \tag{63}$$

The sign of the determinant of the Hessian matrix computed on the periodic orbit, po,

$$\Delta=\left(\tilde{K}^2_{\mathcal{R}\psi}-\tilde{K}_{\mathcal{R}\mathcal{R}}\tilde{K}_{\psi\psi}\right)\Big|_{\rm po}, \tag{64}$$

determines the fate of a perturbation: if Δ is negative it gives the *frequency* of bounded oscillating solutions

$$\omega_p=\frac{1}{q}\sqrt{-\Delta}, \tag{65}$$

where the factor $1/q$ is due to the rescaling from equation (30). If Δ is positive, it gives the characteristic exponent of the time evolution of a growing perturbation

$$\tau=\pm\frac{1}{q}\sqrt{\Delta}. \tag{66}$$

Therefore, with our 1:1 resonant normal form from equation (49), the condition for stability is

$$\Delta=4C^2\mathcal{R}^2\sin^2\psi-2C\left(\mathcal{E}^2+\mathcal{R}^2\right)\times\cos\psi[A-C(2+\cos\psi)]|_{\rm po}<0. \tag{67}$$

Observing that each periodic orbit is identified by a fixed value of the pair $(\psi, \mathcal{R})$ and using the values of the constants in equations (50) and (52), we see that the parameter space is spanned by the ellipticity q and the second integral of motion $\mathcal{E}$; usually, characteristic curves in this space provide the instability threshold. We remark that the choice of the integral $\mathcal{E}$ as one of the coordinates in the parameter space is the simplest one and is usually adopted for a qualitative analysis (Sanders & Verhulst 1985); however, for quantitative predictions and especially for comparisons with other approaches, a more natural choice would be the physical value of the energy E, of which $\mathcal{E}$ (but for a rescaling) is only a first-order approximation. In general, using E in this framework is usually quite difficult for computational problems; this is one of the problems we mentioned above with exploiting the normal form in the normalizing coordinates. Using E with the original Hamiltonian and an approximate integral of motion is instead not only natural but also computationally easier. At the end of this subsection we see how to overcome the problem in the particular case of orbits of type I and how to express the characteristic curves in terms of E.

An immediate application of the condition from equation (67) concerns the inclined and loop orbits discussed above. In cases II and III, we get, respectively,

$$\Delta|_{\psi=0}=2\left(\mathcal{E}^2-\mathcal{R}^2\right)C(A-3C)\quad\text{type II}, \tag{68}$$

$$\Delta|_{\psi=\pi}=2\left(\mathcal{E}^2-\mathcal{R}^2\right)C(C-A)\quad\text{type III}. \tag{69}$$

From the obvious inequality $\mathcal{E}>\mathcal{R}$, $\Delta|_{\psi=0}$ is always positive and $\Delta|_{\psi=\pi}$ is always negative; therefore, the inclined (type II) orbit is unstable for all values of q and $\mathcal{E}$, whereas the loop (type III) orbit (when it exists, compare with the conditions from eqs. [62] and [60]) is stable for all values of q and $\mathcal{E}$.

Our major concern, however, is to analyze the stability properties of type I orbits, the axial orbits, also denoted as *normal modes* because each of them is identified by only one of the actions. Using action-angle variables on the normal mode and Cartesian variables on the normal bundle to it, the ensuing procedure is then first to determine the condition for the normal mode to be a critical curve of the Hamiltonian in these coordinates. Second, to assess its nature (Kummer 1979; Contopoulos 1978; Sanders & Verhulst 1985, § 7.4.4) the condition is found by considering the function

$$K^{(\mu)}=K+\mu\mathcal{H}_0, \tag{70}$$

where μ has to be considered as a *Lagrange multiplier* to take into account that there is the constraint $\mathcal{H}_0=\mathcal{E}$. The Lagrange multiplier is found by imposing

$$dK^{(\mu)}=0, \tag{71}$$

that is, the total differential of equation (70) vanishes on the normal mode. Its nature is assessed by computing the matrix of second derivatives of $K^{(\mu)}$; if the Hessian determinant of the second variation is positive definite, the mode is elliptic stable; if it is negative definite, the mode is hyperbolic unstable. In the case of the y-axis orbit of equation (57), good coordinates are X, P_X, and

$$J=J_2, \tag{72}$$

$$\theta=\theta_2, \tag{73}$$

so that the periodic orbit is given by

$$X=P_X=0,\quad J=\mathcal{E}. \tag{74}$$

The terms in the normal form are then

$$\mathcal{H}_0=(1/2)\left(X^2+P_X^2\right)+J, \tag{75}$$

$$K_2=\frac{1}{2}(q-1)\left(X^2+P_X^2\right)-\frac{3}{32}\left[q\left(X^2+P_X^2\right)^2+\frac{4}{q}J^2\right]-\frac{1}{8}J\left[2\left(X^2+P_X^2\right)+\left(X^2-P_X^2\right)\cos 2\theta+2XP_X\sin 2\theta\right]. \tag{76}$$

It is straightforward to check that, in this case, equation (71) reduced to the periodic orbit defined by equation (74) gives

$$\mu+1-\frac{3\mathcal{E}}{4q}=0, \tag{77}$$

which allows us to find the required value of the Lagrange multiplier. With this result, the matrix of the second derivatives of $K^{(\mu)}$ on the periodic orbit is

$$\frac{1}{8}\begin{pmatrix}s_{11} & -\mathcal{E}\sin 2\theta\\ -\mathcal{E}\sin 2\theta & s_{22}\end{pmatrix}, \tag{78}$$

where

$$s_{11}=4(q-1)-\mathcal{E}[(2+\cos 2\theta)-(3/q)],$$

$$s_{22}=4(q-1)-\mathcal{E}[(2-\cos 2\theta)-(3/q)].$$

The equation $\det[d^2K^{(\mu)}(\mathcal{E})] = 0$ gives

$$(q-1)(4q-3\mathcal{E})\left[4q^2+3\mathcal{E}-q(4+\mathcal{E})\right]=0, \tag{79}$$

and according to the above recipe, for stability this polynomial in $(q, \mathcal{E})$ must be positive. With q in the range from equation (18) as the independent parameter, the instability condition is

$$\frac{4q(1-q)}{3-q} < \mathcal{E} < \frac{4q}{3}. \tag{80}$$

It is interesting to remark that the instability threshold corresponding to the first inequality in equation (80) coincides with the condition of existence of the loop orbit. In fact, from the obvious condition from equation (60) and the values in equation (62), we see that their validity is satisfied exactly by the first inequality in equation (80); this is equivalent to stating that at the point in the parameter space where the short-axis orbits become unstable, the sequence of loop orbits bifurcates. The second inequality corresponds to a return to stability that actually disappears with the higher order treatment.

Proceeding in the same way in the case of the x-axis orbit of equation (56), analogous expressions can be obtained using nonsingular coordinates J, θ, Y, and P_Y, and it is quite straightforward to check that, at this level of approximation, the type Ia orbit is always stable. The procedure above shows the amount of information that can be extracted from the 1:1 resonant normal form. In this respect, it is analogous to the first-order–averaging approach applied by de Zeeuw & Merritt (1983) in studying the Schwarzschild potential.

Before going forward, we want to discuss how to give a more concrete meaning to the result embodied by equation (80); this is possible if the physical energy E appears explicitly. According to the rescaling from equation (30), we assume that

$$nE/\omega_2 \tag{81}$$

is the constant "energy" value assumed by the truncated Hamiltonian K. In the present instance, $n = 1$ and $\omega_2 = 1/q$, so that on the y-axis orbit given by equation (74), we have

$$K = \mathcal{E} - \frac{3}{8q}\mathcal{E}^2 + \ldots = qE. \tag{82}$$

The dots are present to recall that a remainder has been neglected. The series from equation (82) can be inverted to give

$$\mathcal{E} = q\left(E + \frac{3}{8}E^2 + \ldots\right), \tag{83}$$

and this can be used in the treatment of stability to replace $\mathcal{E}$ with E. With this substitution, the critical curve corresponding to the first inequality in equation (80) is simply

$$E(q) = 2(1-q). \tag{84}$$

Equation (82) is also useful for finding the oscillation frequency on the periodic orbit,

$$\kappa_2 = \frac{1}{q}\frac{\partial K}{\partial \mathcal{E}} = \frac{1}{q}\left(1 - \frac{3}{4q}\mathcal{E}\right), \tag{85}$$

which is needed if one is interested in computing either the *frequency ratio*

$$r_2 = \omega_p/\kappa_2, \tag{86}$$

where the perturbation frequency ω_p is defined in equation (65), or the *e-folding rate*

$$\tau_2 = \tau/\kappa_2, \tag{87}$$

where the timescale τ is defined in equation (66).

The analysis with a normal form truncated at higher order would provide more accurate predictions. However, for the time being, we want to first make the analogous analysis with the approximate integral to better understand the relationship between the two approaches.

3.3. *Stability Analysis with the Approximate Integral in the Original Variables*

Recalling the generic expression of the terms in the integral of motion from equation (12), if we truncate to second order, we have

$$I^{(1:1)} = H_0 + \varepsilon^2\left(V_2 - K_2^{(1:1)}\right). \tag{88}$$

This is the best approximate integral of motion of a symmetric perturbed 1:1 oscillator to order ε^4 in the perturbation parameter; in fact, due to the symmetries of the problem odd-degree terms are absent both in the normal form and in the approximate integral. A remark on how to interpret terms in equation (88) is necessary; even if not explicitly indicated, all of them must be intended as polynomials in the original variables (p_x, p_y, x, y). In particular, $K_2^{(1:1)}$ is the same as in equation (34), where capital letter variables are simply replaced by the corresponding lowercase letters.

To assess the stability of periodic orbits, we may proceed in the following way. Starting for definiteness with the y-axis orbit, we use $I^{(1:1)}$ and the conserved energy E to construct an x-p_x Poincaré section by means of the intersection of the function $I^{(1:1)}(x, y, p_x; E)$ with the $y = 0$ hyperplane. The level curves of the function

$$F = I^{(1:1)}(x, 0, p_x; E) \tag{89}$$

allow us to determine the nature of critical points and invariant curves. Critical points (cps) on the surface correspond to periodic orbits in phase space (Contopoulos 2002), and their nature gives the necessary information: they are either extrema (elliptic fixed point = stable periodic orbit) or saddles (hyperbolic fixed point = unstable periodic orbit), and this can be assessed by using the Hessian determinant

$$\left(F_{p_xp_x}F_{xx} - F_{xp_x}^2\right)\Big|_{\rm cp}. \tag{90}$$

Clearly, for a periodic orbit, even the location of the critical points can be already quite difficult, and this limits the generality of the approach. However, in the case of axial orbits, the approach is straightforward; the y-axis orbit, for example, coincides with the origin in this section. The second derivatives at the origin are

$$F_{p_xp_x}|_{\rm cp} = 4(q-1), \tag{91}$$

$$F_{xx}|_{\rm cp} = 4(q-1) + 2E, \tag{92}$$

$$F_{xp_x}|_{\rm cp} = 0. \tag{93}$$

The range of instability (namely, the range where the two nonvanishing second derivatives have different signs) is

$$E > 2(1-q), \tag{94}$$

in agreement with equation (84). We remark that the results reported in Belmonte et al. (2006, cf. Table 1) were obtained just by using both equations (80) and (94) and pointing out the discrepancy between the two predictions. An analogous procedure can be followed for the x-axis orbit by constructing a y-p_y Poincaré section and studying the level curves of the function

$$F = I^{(1:1)}(0, y, p_y; E) \tag{95}$$

obtained by means of the intersection of the function $I^{(1:1)}(x, y, p_y; E)$ with the $x = 0$ hyperplane. In agreement with the results of § 3.2, the x-axis orbit is predicted to be stable using the present critical point analysis.

4. 1:2 SYMMETRIC RESONANCE AND FOURTH-ORDER NORMALIZATION

The loop orbit bifurcates from the y-axis orbit at its instability threshold and is correctly described by the 1:1 (detuned) resonant normal form, because its appearance coincides with the equality of the frequencies of the axial orbit and that of a normal perturbation. The "banana" orbits bifurcate from the x-axis when the frequency of the axial orbit falls to *one-half* of that of a normal perturbation. This is the reason why the 1:1 resonant normal form does not detect any change of stability and we need the 1:2 (detuned) resonant normal form. A detailed study of the orbits in this resonance has been provided by Contopoulos (1963).

4.1. *Orbit Structure of the 1:2 Resonance*

In the case of the $m = 1$, $n = 2$ resonance in the presence of reflection symmetries about both axes, we know that the normal form must be pushed at least to order 4, since it has to include terms of degree $2(m + n) = 6$. Therefore, we have to perform a further step of normalization to include K_4 in the normal form, and the system to solve is now

$$K_2 = V_2 + M_2\mathcal{H}_0, \tag{96}$$

$$K_4 = V_4 + M_2V_2 + M_4\mathcal{H}_0. \tag{97}$$

The expression of the normal form is quite involved (cf. Belmonte et al. 2006), but we can exploit the change of variables to action-angle coordinates as defined in equation (38) to see its structure more easily:

$$K^{(1:2)} = J_1 + 2J_2 + \varepsilon^2[2\delta J_1 - P_2(J_1, J_2)] + \varepsilon^4\left[P_3(J_1, J_2) + \frac{9}{8}J_1^2J_2\cos(4\theta_1 - 2\theta_2)\right], \tag{98}$$

where the polynomials P_2 and P_3 are homogeneous of degree 2 and 3, respectively,

$$P_2 = \frac{3}{4}\left(qJ_1^2 + \frac{1}{q}J_2^2\right) + J_1J_2,$$

$$P_3 = q\left(\frac{5}{6} - \frac{17}{16}q\right)J_1^3 + \left(\frac{13}{12} - \frac{3}{2}q\right)J_1^2J_2 - \left(\frac{5}{12} - \frac{3}{4q}\right)J_1J_2^2 + \frac{29}{96}q^2J_2^3,$$

and the frequency ratio from equation (26) now is

$$\omega_1/\omega_2 = (1/2) + \varepsilon^2\delta. \tag{99}$$

The adapted resonance coordinates are now defined by

$$\psi = 4\theta_1 - 2\theta_2, \tag{100}$$

$$\chi = 4\theta_1 + 2\theta_2, \tag{101}$$

$$J_1 = \mathcal{E} + 2\mathcal{R}, \tag{102}$$

$$J_2 = 2\mathcal{E} - \mathcal{R}. \tag{103}$$

As before, knowledge of the orbit structure is obtained by investigating the fixed points of the one-dimensional dynamical system associated with the effective Hamiltonian

$$\tilde{K}^{(1:2)} = K^{(1:2)}(\mathcal{R}, \psi; \mathcal{E}, q), \tag{104}$$

where

$$\mathcal{R} = \frac{1}{5}(2J_1 - J_2), \tag{105}$$

at fixed values of the integral of motion

$$\mathcal{E} = \frac{1}{5}(J_1 + 2J_2). \tag{106}$$

The study of existence and stability of periodic orbits proceeds in the same way as in § 3. In the present case, the normal modes (axial orbits) are given by

$$\mathcal{R} = 2\mathcal{E}, \quad J_2 = 0 \quad \text{(type Ia)}, \tag{107}$$

$$\mathcal{R} = -\mathcal{E}/2, \quad J_1 = 0 \quad \text{(type Ib)}. \tag{108}$$

The other periodic orbits are identified by the zeros of the system

$$\tilde{K}^{(1:2)}_{\mathcal{R}} = 0, \tag{109}$$

$$\tilde{K}^{(1:2)}_{\psi} = 0. \tag{110}$$

In one case, equation (110) is satisfied by $\psi = 0$, and the corresponding root of equation (109),

$$\mathcal{R} = \mathcal{R}_B(\mathcal{E}, q), \quad J_1 = J_{1(B)}, \quad J_2 = J_{2(B)}, \tag{111}$$

determines the "banana" orbit. In the other case, equation (110) is satisfied by $\psi = \pi$, and the corresponding root of equation (109),

$$\mathcal{R} = \mathcal{R}_A(\mathcal{E}, q), \quad J_1 = J_{1(A)}, \quad J_2 = J_{2(A)}, \tag{112}$$

determines the "antibanana." From equation (106), their range is given by

$$0 \le J_{1(B,A)} \equiv 2\mathcal{R}_{B,A}(\mathcal{E}, q) + \mathcal{E} \le 5\mathcal{E}, \tag{113}$$

$$0 \le J_{2(B,A)} \equiv 2\mathcal{E} - \mathcal{R}_{B,A}(\mathcal{E}, q) \le \frac{5}{2}\mathcal{E}. \tag{114}$$

4.2. *Stability Analysis with the Normal Form*

The procedure to determine the condition of stability of axial orbits leads us to analyze critical curves of the modified function from equation (70), where K is now given by equation (98). From the analysis of the 1:1 resonance, we have seen that it cannot detect any instability threshold of the long-axis periodic orbit, and

therefore, we readily address this question in the framework of the 1:2 resonance. Considering the x-axis (type Ia, eq. [107]) orbit, good coordinates are given by

$$X = \sqrt{2J}\cos\theta, \tag{115}$$

$$P_X = \sqrt{2J}\sin\theta, \tag{116}$$

$$Y = Y, \tag{117}$$

$$P_Y = V, \tag{118}$$

so that the periodic orbit is given by

$$Y = V = 0, \quad J = 5\mathcal{E}, \tag{119}$$

$$\mathcal{H}_0 = J + Y^2 + V^2. \tag{120}$$

Equation (71) allows us to find the Lagrange multiplier

$$\mu = \frac{1}{16}\left(-32q + 24\mathcal{E}q - 40\mathcal{E}^2 q + 51\mathcal{E}^2 q^2\right). \tag{121}$$

The equation $\det[K^{(\mu)}(\mathcal{E})] = 0$, obtained by computing the matrix of the second derivatives of $K^{(\mu)}$ on the normal bundle to the periodic orbit from equation (119), is

$$\left[48 - 96q + 24(3q-1)\mathcal{E} + \left(26 - 153q + 153q^2\right)\mathcal{E}^2\right] \times \left[48 - 96q + 24(3q-1)\mathcal{E} + \left(26 - 159q + 153q^2\right)\mathcal{E}^2\right] = 0, \tag{122}$$

whose zeros are

$$\mathcal{E}_{B\pm} = 4\frac{3 - 9q \pm \sqrt{3}\sqrt{-23 + 187q - 432q^2 + 306q^3}}{26 - 153q + 153q^2}, \tag{123}$$

$$\mathcal{E}_{A\pm} = 4\frac{3 - 9q \pm \sqrt{3}\sqrt{-23 + 193q - 444q^2 + 306q^3}}{26 - 159q + 153q^2}. \tag{124}$$

It happens that the conditions of existence in equations (113) and (114) are satisfied exactly when

$$\mathcal{E}_{B+} \le \mathcal{E} \le \mathcal{E}_{B-} \tag{125}$$

for the banana orbit and

$$\mathcal{E}_{A+} \le \mathcal{E} \le \mathcal{E}_{A-} \tag{126}$$

for the antibanana. We again see the relation between transition to instability of a normal mode and bifurcation of a resonant periodic orbit, since outside the above ranges, the determinant $\Delta = \det[K^{(\mu)}(\mathcal{E})]$ is positive. As before, we want to make the analogous analysis with the approximate integral to better grasp the relationship between the two approaches.

4.3. *Stability Analysis with the Approximate Integral of Motion*

We can develop the parallel approach of determining the nature of fixed points on the surface of section also for higher order approximate integrals. Using equation (12), if we truncate at fourth order, we have

$$I^{(1:2)} = H_0 + \varepsilon^2(V_2 - K_2) + \varepsilon^4(V_4 - \{g_2, K_2\} - K_4), \tag{127}$$

where

$$g_2 = \frac{1}{24}P_X^2 P_Y Y - \frac{3q}{16}P_X^3 X - \frac{1}{3}P_X P_Y^2 X - \frac{5q}{16}P_X X^3 - \frac{3}{32q}P_Y^3 Y - \frac{7}{24}P_Y X^2 Y - \frac{1}{6}P_X X Y^2 - \frac{5}{32q}P_Y Y^3 \tag{128}$$

is the second-order generating function determined in the first step of the normalization. This is the best approximate integral of motion of a symmetric perturbed 1 : 2 oscillator to order ε^6 in the perturbation parameter. Let us again consider the x-axis orbit; the construction of the y-p_y Poincaré section and the study of the critical points of the function

$$F = I^{(1:2)}(0, y, p_y; E), \tag{129}$$

obtained by means of the intersection of the function $I^{(1:2)}(x, y, p_y; E)$ with the $x = 0$ hyperplane, proceeds as above. Concerning the nature of the fixed point in the origin, we get quadratic inequalities in the energy analogous to those arising from equation (122); the discrepancy between the two methods is still of order δ^2. The locus of points where the origin in the y-p_y Poincaré section changes from an extremum to a saddle are

$$E_{B\pm} = 4\frac{-8 + 10q^2 \pm \sqrt{228q - 887q^2 + 830q^3 + 100q^4}}{-76 + 165q^2}, \tag{130}$$

$$E_{A\pm} = 4\frac{-4 + 2q^2 \pm \sqrt{180q - 659q^2 + 614q^3 + 4q^4}}{15(-4q + 7q^2)}. \tag{131}$$

These are clearly related to those found above, but are not the same; to reconcile the two predictions, it is first necessary to give the relation between the new "energy" $\mathcal{E}$ and the physical energy E. But this is actually not enough; as seen in the 1:1 case, one must also perform a series expansion of the relations in the (q, E)-plane and truncate it at the same order as the normal form.

According to the rescaling from equation (30), with $n = 2$ and $\omega_2 = 1/q$, on the x-axis orbit given by equation (119), we have

$$K = 2qJ - \frac{3}{4}qJ^2 + \frac{1}{2}q\left[\frac{5}{3} - \frac{17}{4}q(q-1)\right]J^3 + \ldots = 2qE. \tag{132}$$

The dots are present to recall that a remainder has been neglected. The series from equation (132) can be inverted to give

$$J = 5\mathcal{E} = E + \frac{3}{8}E^2 - \frac{1}{16}\left[\frac{13}{6} + 17q(1-q)\right]E^3 + \ldots, \tag{133}$$

and this can be used in the treatment of stability to replace $\mathcal{E}$ with E. We limit ourselves to the lower bounds in the ranges in equations (125) and (126), getting *sufficient* conditions for the bifurcation of, respectively, bananas and antibananas:

$$E_{B+} = 8\left(q - \frac{1}{2}\right) - \frac{20}{3}\left(q - \frac{1}{2}\right)^2, \tag{134}$$

$$E_{A+} = 8\left(q - \frac{1}{2}\right) + \frac{28}{3}\left(q - \frac{1}{2}\right)^2. \tag{135}$$

It can be checked by a long but easy computation that the above series coincide with those obtained by, respectively, expanding E_{B+} in equation (130) and E_{A+} in equation (131) in q around $q = 1/2$, thus confirming the equivalence between the two methods. In § 5 we present a more precise result obtained from a normal form truncated at higher order.

5. ORBIT STRUCTURE OF THE LOGARITHMIC POTENTIAL

The theory discussed in the above sections is applied to investigate the orbit structure of the logarithmic potential. In particular, we are interested in simple recipes to predict the stability of the main periodic orbits. We can compare these analytical predictions with other results, mainly numerical, from the literature. In particular, we have chosen the work by Miralda-Escudé & Schwarzschild (1989, hereafter MES89), who made an accurate numerical exploration of the phase-space structure of the logarithmic potential; they give the existence parameter ranges of the main families of periodic orbits and the bifurcation ensuing from instability thresholds in two models (corresponding to ellipticity values $q = 0.7$ and 0.9) determined by solving the perturbation equations with the Floquet method. The authors used the core radius R_c to parameterize the sequence of periodic orbits, because they were interested in comparing the results with the case of the *singular* scale-free case $R_c = 0$; in fact, they fix the energy $E = 0$ in all their computations and vary R_c and q. For our purposes, it is more natural to use the energy and the ellipticity as parameters. To compare our results with that in MES89, the conversion

$$E = -\log R_c \tag{136}$$

must be used. We have numerically computed the instability thresholds of the axial orbits in the range $0.6 < q < 1$, with results in agreement with MES89 where available.

Another approach to the study of the stability of axial orbits in the logarithmic potential has been followed by Scuflaire (1995, hereafter S95), who solved the Hill-like equation of the normal perturbation to the periodic orbit by means of a Poincaré-Lindstedt series expansion up to order 20. S95 uses a, the amplitude of the axial orbit, as a parameter; the conversion to energy is given by

$$E = (1/2)\log\left(1 + a^2\right), \tag{137}$$

$$E = (1/2)\log\left[1 + (a/q)^2\right], \tag{138}$$

on the x-axis and y-axis orbits, respectively. The approach in S95 is analytical and perturbative, but being based on the theory of nonlinear differential equations with periodic coefficients (Jordan & Smith 1999), is quite different from ours; it is therefore a very useful term of comparison, because its results, even if restricted to axial orbits only, stem from a very high order perturbation analysis.

5.1. *Stability and Bifurcation of Closed Orbits*

To get a higher precision than that obtained in the discussion of §§ 3 and 4, we have computed the 1:1 and 1:2 resonant normal form up to order 6 (degree 8 in the variables). A general analysis of these normal forms is quite cumbersome, but concerning the axial orbits, they allow us to get quite easily improved predictions of the stability thresholds.

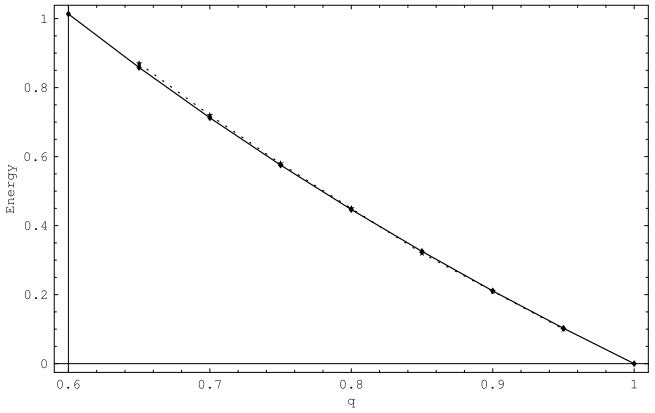

FIG. 1.—Stability thresholds of the short y-axis orbit: analytical (eq. [144], *solid line*); numerical solution with the Floquet method (*dotted line*).

In the case of the y-axis orbit, using the same coordinate as in § 3.2, the normal form on the periodic orbit ($J_1 = 0, J_2 = \mathcal{E}$) is

$$K = \mathcal{E} - \frac{3}{8q}\mathcal{E}^2 + \frac{29}{192q^2}\mathcal{E}^3 - \frac{55}{1024q^3}\mathcal{E}^4 + \ldots = qE. \tag{139}$$

As a consequence, the upgraded evaluation of the frequency on the y-axis orbit is

$$\kappa_2(\mathcal{E}) = \frac{1}{q}\frac{\partial K}{\partial \mathcal{E}} = \frac{1}{q}\left(1 - \frac{3}{4q}\mathcal{E} + \frac{29}{64q^2}\mathcal{E}^2 - \frac{55}{256q^3}\mathcal{E}^3\right). \tag{140}$$

These series generalize equations (82) and (85), respectively. As before, we actually prefer to have expressions in terms of the "real" energy E, so we invert equation (139) to get

$$\mathcal{E} = qE\left(1 + \frac{3}{8}E + \frac{25}{192}E^2 + \frac{35}{1024}E^3 + \ldots\right) \tag{141}$$

and substitute in equation (140), obtaining

$$\kappa_2(E) = \frac{1}{q}\left(1 - \frac{3}{4}E + \frac{11}{64}E^2 + \frac{7}{256}E^3\right). \tag{142}$$

Computing the determinant of the matrix of the second derivatives of the modified function from equation (70), $\det\left[d^2K^{(\mu)}(\mathcal{E})\right]$, and setting it equal to zero gives

$$(q-1)\left[64q^2 - 48q\mathcal{E} + (29 - 17q)\mathcal{E}^2\right] \times \left[64q^2(1+q) + 16q(3-q)\mathcal{E} - \left(q^2 - 2q + 29\right)\mathcal{E}^2\right] = 0, \tag{143}$$

generalizing equation (79). Substituting equation (141) and solving for E, we get

$$E(q) = 2(1-q) + (1-q)^2 - \frac{5}{6}(1-q)^3, \tag{144}$$

obtaining a prediction of the stability-instability transition of the short-axis orbit (with subsequent bifurcation of the loop orbit) up to third order in the (q, E)-plane. The values obtained from this relation are shown in Figure 1 (*solid line*) and are compared with the numerical results from the Floquet theory (*dotted line*), showing a very good agreement; the values obtained by MES89 (*dots*) are

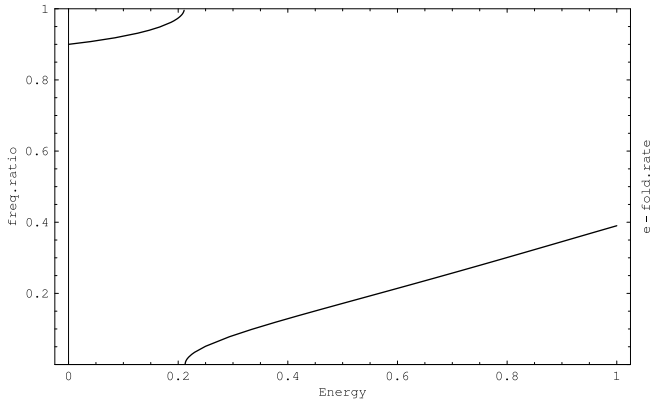

FIG. 2.—Frequency ratio and e-folding rate for the short y-axis orbit at $q = 0.9$.

0.21 in the case of $q = 0.9$ and 0.72 in the case of $q = 0.7$. Moreover, the expansions from equations (142) and (144) coincide up to the same order with those reported in S95 when the conversion from amplitude to energy is performed using equation (138).

We may also compute the ratio from equation (86) between the frequency of the perturbation and that of the periodic orbit, where the perturbation frequency is associated with the determinant in the left-hand side of equation (143) like in equation (65) and the e-folding rate is as defined in equation (87); as expected, at low energy the ratio has limit q, since $\omega_p \to 1$ and $\kappa_2 \to 1/q$, whereas at the transition, the ratio coincides with the resonance value 1. In Figure 2 the two quantities are plotted for $q = 0.9$, and in Figure 3 they are plotted for $q = 0.7$. They can be compared with the corresponding figures in MES89 (bottom panels in their Figs. 7 and 8) where they have been obtained numerically. The return to stability at higher energies mentioned in § 3 (cf. the second inequality in eq. [80]) does not occur in the logarithmic potential. This incompleteness also appears in the treatment made by de Zeeuw & Merritt (1983) of the Schwarzschild potential using first-order averaging. This problem is solved by our higher order approach, because the other roots of equation (143) are either negative or complex.

In the case of the x-axis orbit, we limit ourselves to provide results without derivation. The 1:2 normal form on the periodic orbit (eq. [98] with $J_2 = 0$) is

$$K = 2qJ_1 - \frac{3}{4}qJ_1^2 + \frac{1}{2}q\left[\frac{5}{3} - \frac{17}{4}q(q-1)\right]J_1^3 - \frac{5}{16}q\left(\frac{7}{2} - 11q - \frac{75}{8}q^2\right)J_1^4. \quad (145)$$

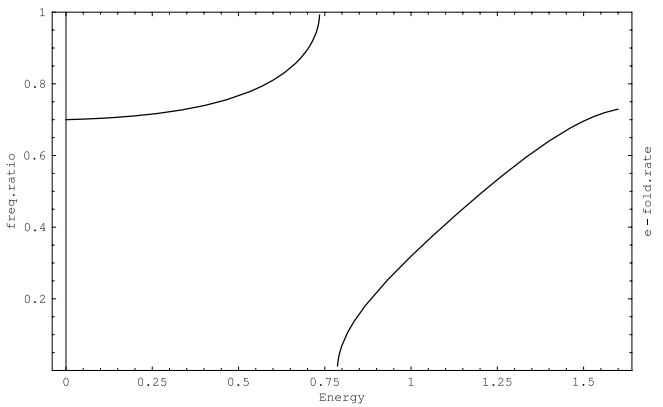

FIG. 3.—Same as Fig. 2, but for $q = 0.7$.

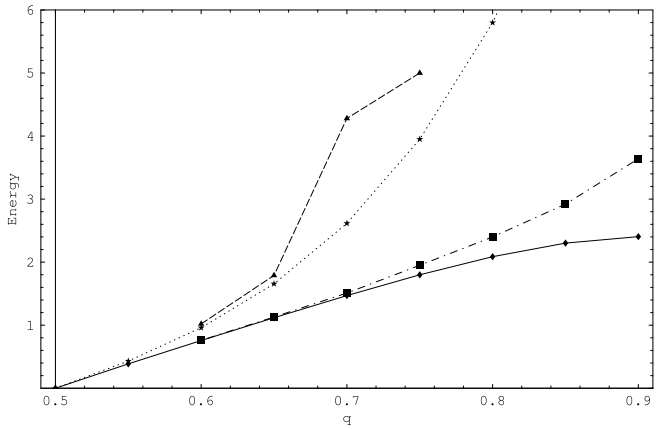

FIG. 4.—Stability thresholds of the long x-axis orbit: analytical (banana bifurcation, eq. [149], *solid line*; and antibanana bifurcation, eq. [150], *dotted line*) and numerical (*dash-dotted and dashed lines, respectively*).

As a consequence, the upgraded evaluation of the expansion of the action in terms of the true energy is

$$J_1 = E + \frac{3}{8}E^2 - \frac{1}{16}\left[\frac{13}{6} + 17q(1-q)\right]E^3 + \frac{5}{128}\left(\frac{3}{4} + 7q - \frac{27}{2}q^2\right)E^4. \quad (146)$$

The frequency on the x-axis orbit computed through

$$\kappa_1(J_1) = \frac{1}{2q}\frac{\partial K}{\partial J_1} \quad (147)$$

and expressed in term of the upgraded expansion from equation (146) is

$$\kappa_1 = 1 - \frac{3}{4}E + \frac{11}{64}E^2 + \frac{7}{256}E^3. \quad (148)$$

Computing the determinant of the matrix of the second derivatives of the modified function from equation (70) on the periodic orbit, $\Delta = \det[d^2K^{(\mu)}]$, and setting it equal to zero gives, in this case, an equation of sixth degree; the two roots in addition to those in equations (130) and (131), in analogy to the roots E_{B-} and E_{A-}, does not put further constraints on the conditions sufficient for instability of the axial orbit. Therefore, we use the upgraded version of the relevant roots and express them as series in powers of $q - \frac{1}{2}$, to get

$$E_{B+} = 8\left(q - \frac{1}{2}\right) - \frac{20}{3}\left(q - \frac{1}{2}\right)^2 + \frac{268}{9}\left(q - \frac{1}{2}\right)^3, \quad (149)$$

$$E_{A+} = 8\left(q - \frac{1}{2}\right) + \frac{28}{3}\left(q - \frac{1}{2}\right)^2 + \frac{460}{9}\left(q - \frac{1}{2}\right)^3, \quad (150)$$

obtaining a prediction of the stability-instability transition of the long-axis orbit (with subsequent bifurcation of the banana orbit) up to third order in the (q, E)-plane. The values obtained from these relations are shown in Figure 4; the solid and dotted lines are, respectively, the relations in equations (149) and (150) and are compared with the numerical results from the Floquet theory, namely, bifurcation of the banana (*dash-dotted line*) and bifurcation of the antibanana (*dashed line*). The values obtained by MES89 are, respectively, $E = 1.52$ and 4.29 in the case

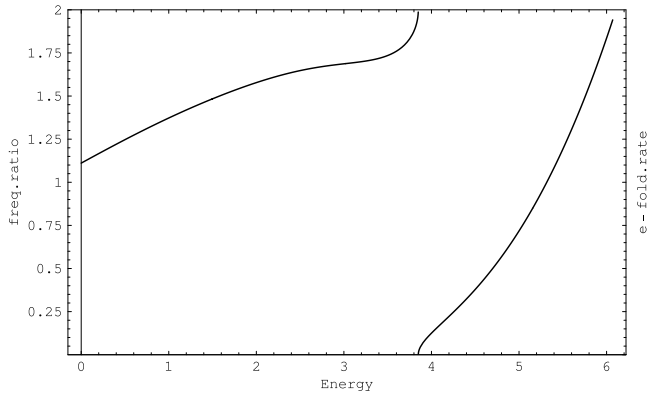

FIG. 5.—Same as Fig. 2, but for the long x-axis orbit.

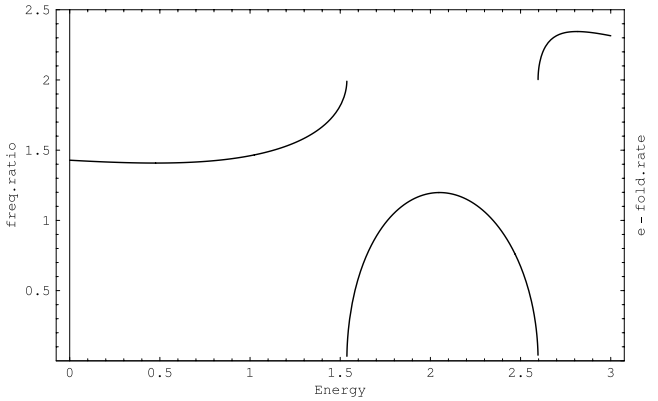

FIG. 6.—Same as Fig. 6, but for $q = 0.7$.

$q = 0.7$, whereas in the case $q = 0.9$, only the first transition at $E = 3.62$ is available. Moreover, the expansions from equations (148)–(150) coincide up to the same order with those reported in S95 when the conversion from amplitude to energy is performed using equation (137).

We may also compute the ratio

$$r_1 = \omega_p/\kappa_1, \tag{151}$$

between the frequency of the perturbation and that of the periodic orbit, where the perturbation frequency is associated with the determinant on the left-hand side of equation (122) like in equation (65) and the e-folding rate is as defined in equation (87), but with κ_1 in place of κ_2. In this case, at low energy the ratio has limit $1/q$, since $\omega_p \to 1/q$ and $\kappa_1 \to 1$, whereas at the transition, the ratio has the resonance value 2. In Figure 5 the two quantities are plotted for $q = 0.9$, and in Figure 6 they are plotted for $q = 0.7$. They can be compared with the corresponding figures in MES89 (top panels in their Figs. 7 and 8) where they have been obtained numerically.

A demanding test of an analytical approach like that based on normal forms is that of investigating higher order boxlets; actually, the procedure is analogous to that above, but the number of terms in the normal form can be very high. We have limited ourselves to investigating the bifurcation of fish orbits. To this end, we have to compute the 2 : 3 symmetric normal form, which must include terms of degree at least $2(2 + 3) = 10$. Once $K^{(2:3)}$ is obtained, we can express it in adapted resonance coordinates

$$\psi = 6\theta_1 - 4\theta_2, \tag{152}$$

$$\chi = 6\theta_1 + 4\theta_2, \tag{153}$$

$$J_1 = 2\mathcal{E} + 3\mathcal{R}, \tag{154}$$

$$J_2 = 3\mathcal{E} - 2\mathcal{R}, \tag{155}$$

and as before, knowledge of the orbit structure is obtained by investigating the fixed points of the one-dimensional dynamical system associated with the effective Hamiltonian

$$\tilde{K}^{(2:3)} = K^{(2:3)}(\mathcal{R}, \psi; \mathcal{E}, q). \tag{156}$$

The periodic orbits are identified by the zeros of the system

$$\tilde{K}^{(2:3)}_{\mathcal{R}} = 0, \tag{157}$$

$$\tilde{K}^{(2:3)}_{\psi} = 0. \tag{158}$$

In particular, equation (158) is satisfied by $\psi = 0$, and the corresponding root of equation (157)

$$\mathcal{R} = \mathcal{R}_F(\mathcal{E}, q) \tag{159}$$

determines the "fish" orbit. Using this relation and equation (154) in the existence condition $0 \le J_{1F} \le 2\mathcal{E}$ gives an equation whose roots are related to the bifurcation of the fish orbit from the normal mode. Using as usual the true energy in place of the fictitious $\mathcal{E}$, we get the fourth-degree equation

$$\sum_{i=0}^{4} c_i(q) E^i = 0, \tag{160}$$

with coefficients

$$c_0 = -6 + 9q,$$

$$c_1 = 3 - \frac{27q}{4},$$

$$c_2 = -\frac{381}{500} + \frac{54{,}639q}{4000} - \frac{677{,}727q^2}{16000} + \frac{14{,}337q^3}{256} - \frac{12{,}393q^4}{512},$$

$$c_3 = \frac{637}{250} - \frac{3186q}{125} + \frac{705{,}807q^2}{8000} - \frac{131{,}787q^3}{1024} + \frac{66{,}339q^4}{1024},$$

$$c_4 = -\frac{18{,}689}{12{,}800} + \frac{4{,}279{,}197q}{256{,}000} + \frac{28{,}267{,}497q^2}{7{,}168{,}000} - \frac{15{,}582{,}699q^3}{102{,}400} + \frac{1{,}062{,}755{,}397q^4}{3{,}276{,}800} - \frac{1{,}370{,}678{,}193q^5}{4{,}096{,}000} + \frac{6{,}134{,}535q^6}{32{,}768} - \frac{5{,}688{,}387q^7}{131{,}072}.$$

Equation (160) has a complex pair and a real pair of solutions; the smaller positive root can be used for our purposes as a prediction of the bifurcation energy. For $q = 0.7$ and 0.9, we get $E_F = 0.2$ and 1.7, respectively. The bifurcation energies numerically found in MES89 are $E_F = 0.21$ and 2.28, respectively; clearly, the disagreement between the theoretical and numerical results rapidly grows with detuning.

5.2. *Phase-Space Fraction Occupied by Boxlets*

An analytical estimate of the fraction of phase space occupied by each orbit family can be made with the tools constructed so far. The method is based on the computation of the area on the surface of section associated with the given orbit family. In this respect, the estimate is affected by an error due to neglecting a factor

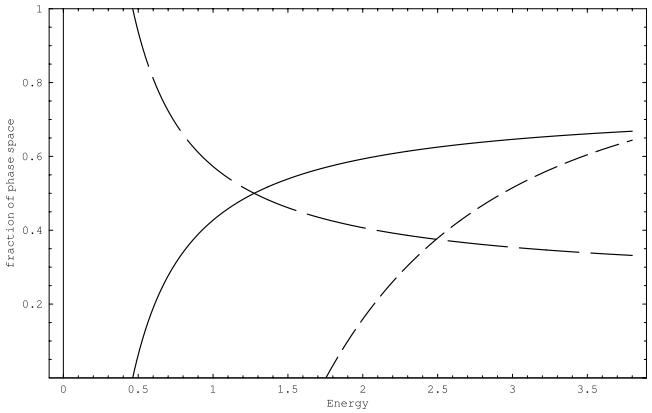

FIG. 7.—Fraction of phase space occupied by low-order boxlets at $q = 0.7$: loops (*solid line*), boxes (*long-dashed line*), and bananas (*short-dashed line*).

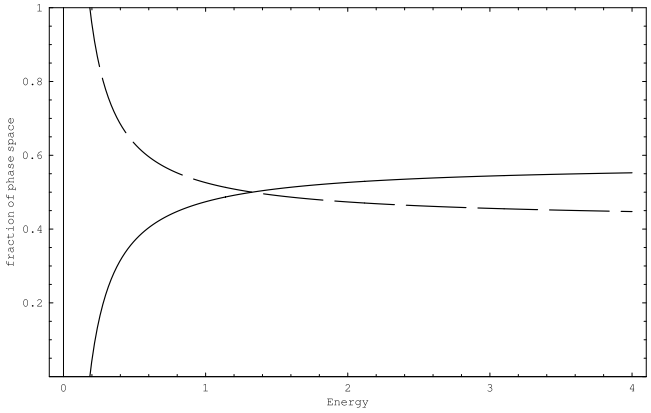

FIG. 8.—Fraction of phase space occupied by low-order boxlets at $q = 0.9$: loops (*solid line*) and boxes (*dashed line*).

depending on the period of individual orbits; this factor in general does not allow us to assume simple proportionality between volumes in phase space and areas on the surface of section (Binney et al. 1985). However, in our case, the periods of the families at hand belong to a range small enough to produce a negligible effect. To illustrate the method in its simplest form, we use the lowest order theory applied to loop orbits in § 3 and to bananas in § 4.

For the loop orbits, we have that equation (62) gives the values of the actions in terms of $\mathcal{E}$ and q. As usual, to compare with quantities of the "real" system, we need to convert to the physical energy, and this can be done by means of the K on the loop

$$K^{(1:1)}\big|_{\rm III} = \frac{q\left[(1+q)\mathcal{E} - \mathcal{E}^2 + 2(q-1)^2\right]}{3q^2 - 2q + 3} = qE. \qquad (161)$$

Inverting and expanding, this gives the integral $\mathcal{E} = \mathcal{E}(E)$ in terms of the true energy. An important point to remark on is that the J terms appearing in the general expression of the normal form, e.g., $K^{(1:1)}$ of equation (37), are not true actions along a given family. However, the J terms in equation (62) *are* true actions; in particular, at the bifurcation of the loop from the axial orbit they are the actions of the orbits asymptotic (*homoclinic*) to the y-axis orbit, the "first" loop and the "last" box, respectively. Therefore, $J_1(E)|_{\rm III}$ is the area inside the homoclinic orbit on the x-p_x surface of section, and $J_2(E)|_{\rm III}$ is the area inside the homoclinic orbit on the y-p_y surface of section. The ratios

$$f_{\rm loop} = \frac{J_1(E)|_{\rm III}}{\mathcal{E}(E)}, \quad f_{\rm box} = \frac{J_2(E)|_{\rm III}}{\mathcal{E}(E)} \qquad (162)$$

can therefore be used as an approximation of the fraction of phase space occupied by the loops and the boxes, respectively. Substituting into equation (62) and dividing by $\mathcal{E}(E)$, their expressions are

$$f_{\rm loop} = \frac{2(-3 + 3q - 5q^2 + 5q^3) + E(9 - 9q + 11q^2 - 3q^3)}{(3 - 2q + 3q^2)\left[-2(1-q)^2 + E(3 - 2q + 3q^2)\right]}, \qquad (163)$$

$$f_{\rm box} = \frac{q[10 - 10q + 6q^2 - 6q^3 + E(-3 + 11q - 9q^2 + 9q^3)]}{(3 - 2q + 3q^2)\left[-2(1-q)^2 + E(3 - 2q + 3q^2)\right]}. \qquad (164)$$

In Figures 7 and 8 the two quantities are plotted for $q = 0.7$ and 0.9, respectively, and a comparison can be made with the numerical estimate of $f_{\rm loop}$ in MES89 (cf. their Fig. 10) computed by applying an approximate version of the recipe by Binney et al. (1985). We remark that with their approach MES89 are not able to compute the fraction pertaining to boxes, since their method does not use families associated with normal modes.

Concerning banana orbits, we may follow an analogous line of reasoning, obtaining

$$f_{\rm ban} = \frac{J_{1(B)}(E)}{\mathcal{E}(E)}, \qquad (165)$$

where $J_{1(B)}$, introduced in equation (111), can be interpreted as the area inside the orbit homoclinic to the unstable fixed point on the x-p_x surface of section. In Figure 7 this quantity is plotted for $q = 0.7$, whereas for $q = 0.9$, its application is meaningless because it concerns exceedingly high energies. Comparing with the numerical estimate of $f_{\rm ban}$ in MES89 (cf. left panel of their Fig. 10), we have to take into account that our analytical estimates originate from two independent systems, the two normal forms

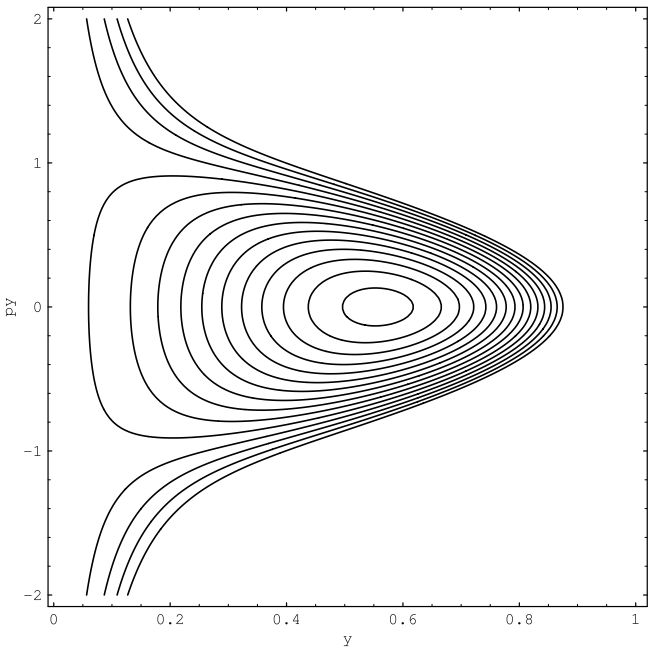

FIG. 9.—Zero-energy y-p_y surface of the section of the singular logarithmic potential with $q = 0.7$, computed with the 1 : 1 resonant normal form.

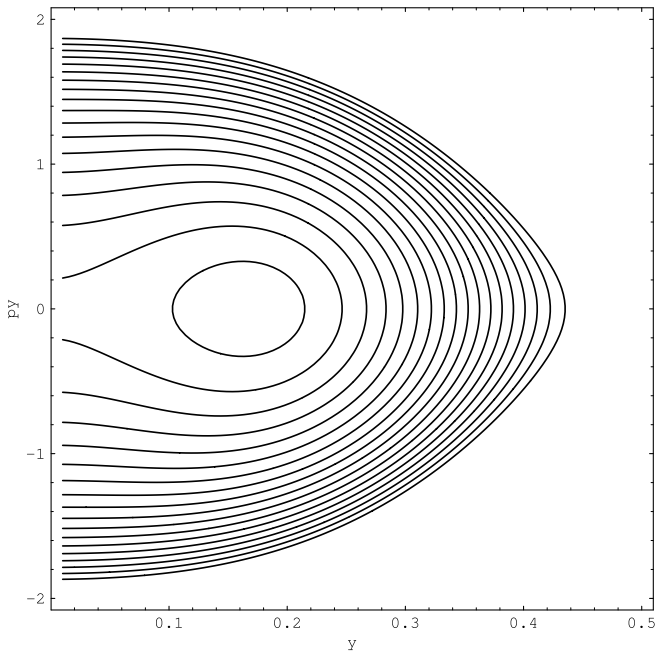

FIG. 10.—Same as Fig. 9, but for the 1 : 2 resonant normal form.

based on the 1:1 and 1 : 2 resonances. Therefore, we cannot expect that the occupancies of each family sum up to give the whole phase space. A suitable normalization would be necessary to adjust the proportions and could account for the numerical result. However, since the normalization process contains a certain degree of arbitrariness, we leave the quantities as they are and use them only as relative measures. We come again to this point in the § 5.3.

5.3. *Surface of Section for Singular Logarithmic Potential*

It is tempting to try to extract information concerning the scale-free singular limit of the logarithmic potential from our analytical setting based on series expansions. Formally, this operation should be hindered by the lack of a series representation of the singular logarithmic potential. However, we may nonetheless "force" our approximate integrals of motion to play their role in the singular limit too. If we try our chance by constructing, e.g., the y-p_y surface of section with the same procedure as in § 4.3, using now

$$\frac{1}{2}\left(p_x^2 + p_y^2\right) + \frac{1}{2}\log\left(x^2 + \frac{y^2}{q^2}\right) = 0 \qquad (166)$$

to eliminate p_x, we get, quite surprisingly, acceptable results. In Figure 9 we see the section obtained by using the approximate integral $I^{(1:1)}$ of equation (88) for $q = 0.7$; it gives the family of loops around the stable periodic orbit at $y \simeq 0.56$ and can be compared with Figure 1 in MES89. In Figure 10 we see the section obtained by using the approximate integral $I^{(1:2)}$ of equation (127), again for $q = 0.7$; it gives the family around the stable banana at $y \simeq 0.16$ and boxes around it. A comparison with the same Figure 1 in MES89 shows that also the banana is located quite well on the section. However, from these considerations emerge the main limitation of the approach based on resonant normal forms: *each resonance captures only one feature* of the system under study. For example, comparing our Figures 9 and 10 with a numerically computed section like that in Figure 1 in MES89, we see that, in the "true" system, the island around the banana "eats" a substantial part of the island around the closed loop. A reliable description of this phenomenon is not possible in the framework of a *single-resonance* theory. This remark is evidently related to the interpretation of the previous results concerning the computation of the fractions in phase space.

6. CONCLUSIONS

We have applied the method of resonant detuned normal forms to investigate relevant features of a nonintegrable potential of interest in galactic dynamics. The analytical setup consists of constructing a new integrable system (the "normal form") by means of a sequence of canonical transformations with the method of the Lie transform. The algorithm can be put in an efficient and powerful form (Boccaletti & Pucacco 1999; Giorgilli 2002) which can handle quite high-order expansions. We have shown how to exploit resonant normal forms to extract information on several aspects of the dynamics of the original system. In particular, using energy and ellipticity as parameters, we have computed the instability thresholds of axial orbits, bifurcation values of low-order boxlets, and phase-space fractions pertaining to the families around them. We have also shown how to infer something about the singular limit of the potential.

As in any analytical approach, this method has the virtue of embodying in (more or less) compact formulae simple rules to compute specific properties, giving a general overview of the behavior of the system. In the case in which a nonintegrable system has a regular behavior in a large portion of its phase space, a very conservative strategy like the one adopted in this work provides sufficient qualitative and quantitative agreement with other more accurate but less general approaches. In our view, the most relevant limitation of this approach, common to all perturbation methods, comes from the intrinsic structure of the single-resonance normal form. The usual feeling about the problems posed by nonintegrable dynamics is in general grounded in trying to cope with the interaction of (several) resonances. Each normal form is instead able to correctly describe only one resonance at a time. However, we remark that the regular dynamics of a nonintegrable system can be imagined as a superposition of very weakly interacting resonances. If we are not interested in the thin stochastic layers in the regular regime, each portion of phase space associated with a given resonance has a fairly good alias in the corresponding normal form. An important subject of investigation would therefore be that of including weak interactions in a sort of higher order perturbation theory. For the time being, there are two natural lines of development of this work: (1) to extend the analysis to cuspy potentials and/or central "black holes" and (2) to apply this normalization algorithm to systems with 3 degrees of freedom.

REFERENCES

Belmonte, C., Boccaletti, D., & Pucacco, G. 2006, Celest. Mech. Dyn. Astron., 95, 101
Binney, J. 1981, MNRAS, 196, 455
Binney, J. Gerhard, O. E., & P. Hut, 1985, MNRAS, 215, 59
Binney, J., & Spergel, D. 1982, ApJ, 252, 308
Binney, J., & Tremaine, S. 1987, Galactic Dynamics (Princeton: Princeton Univ. Press)
Birkhoff, G. D. 1927, Dynamical Systems, Vol. 9 (New York: American Mathematical Society)
Boccaletti, D., & Pucacco, G. 1999, Theory of Orbits, Vol. 2 (Berlin: Springer)
Contopoulos, G. 1963, AJ, 68, 763
———. 1965, AJ, 70, 817
———. 1970, AJ, 75, 96
———. 1978, Celest. Mech. Dyn. Astron., 18, 195

Contopoulos, G. 2002, Order and Chaos in Dynamical Astronomy (Berlin: Springer)
Contopoulos, G., Efthymiopoulos, C., & Giorgilli, A. 2003, J. Phys. A, 36, 8639
Dehnen, W. 1993, MNRAS, 265, 250
Deprit, A. 1969, Celest. Mech., 1, 12
de Zeeuw, T., & Merritt, D. 1983, ApJ, 267, 571
Dragt, A., & Finn, J. M. 1976, J. Mathematika Phys., 17, 2215
Efthymiopoulos, C., Giorgilli, A., & Contopoulos, G. 2004, J. Phys. A, 37, 10831
Finn, J. M. 1986, in Local and Global Methods of Nonlinear Dynamics, ed. A. W. S'enz, W. W. Zachary, & R. Cawley (Berlin: Springer), 63
Fridman, T., & Merritt, D. 1997, AJ, 114, 1479
Gerhard, O., & Saha, P. 1991, MNRAS, 251, 449
Giorgilli, A. 2002, Notes on Exponential Stability of Hamiltonian Systems (Pisa: Centro di Ricerca Matematica E)
Gustavson, F. 1966, AJ, 71, 670
Hori, G. I. 1966, PASJ, 18, 287
Jordan, D. W., & Smith, P. 1999, Nonlinear Ordinary Differential Equations (Oxford: Oxford Univ. Press)
Kaasalainen, M., & Binney, J. 1994a, MNRAS, 268, 1033
———. 1994b, Phys. Rev. Lett., 73, 2377
Koseleff, P. V. 1994, Celest. Mech. Dyn. Astron., 58, 17
Kummer, M. 1979, in Stochastic Behavior in Classical and Quantum Hamiltonian Systems, ed. G. Casati & J. Ford (Berlin: Springer), 57
Merritt, D. 1999, PASP, 111, 129
Merritt, D., & Valluri, M. 1996, ApJ, 460, 136
Meyer, K. R., & Hall, G. R. 1992, Introduction to Hamiltonian Dynamical Systems and the N-Body Problem (Berlin: Springer)
Miralda-Escudé, J., & Schwarzschild, M. 1989, ApJ, 339, 752 (MES89)
Moser, J. 1968, Mem. Am. Math. Soc., 81, 1
Papaphilippou, Y., & Laskar, J. 1996, A&A, 307, 427
———. 1998, A&A, 329, 451
Sanders, J. A., & Verhulst, F. 1985, Averaging Methods in Nonlinear Dynamical Systems (New York: Springer)
Schwarzschild, M. 1979, ApJ, 232, 236
Scuflaire, R. 1995, Celest. Mech. Dyn. Astron., 61, 261 (S95)
Sridhar, S., & Touma, J. 1997, MNRAS, 287, L1
Tuwankotta, J. M., & Verhulst, F. 2000, SIAM J. Appl. Math., 61, 1369
Verhulst, F. 1996, Nonlinear Differential Equations and Dynamical Systems (Berlin: Springer)
Yanguas, P. 2001, Nonlinearity, 14, 1
Zhao, H. S., Carollo, C. M., & De Zeeuw, T. 1999, MNRAS, 304, 457